Comparative studies of Escherichia coli strains using different glucose uptake systems: metabolism and energetics

Chen, R.; Yap, W.M.G.J.; Postma, P.W.; Bailey, J.E.

Publication date
1997

Published in
Biotechnology and Bioengineering

Comparative Studies of *Escherichia coli* Strains Using Different Glucose Uptake Systems: Metabolism and Energetics

Ruizhen Chen,[1]* Wyanda M. G. J. Yap,[2] Pieter W. Postma,[2] James E. Bailey[3]

[1]Department of Chemical Engineering, California Institute of Technology, Pasadena, California 91125
[2]E. C. Slater Institute, University of Amsterdam, Plantage Muidergracht 12, 1018 TV Amsterdam, The Netherlands
[3]Institute of Biotechnology, ETH Zürich, CH-8093-Zürich, Switzerland; telephone: 411 633 31 70; fax: 411 633 10 51; e-mail: jay@biotech.biol.ethz.eh

Received 9 May 1996; accepted 8 July 1997

Abstract: Modifying substrate uptake systems is a potentially powerful tool in metabolic engineering. This research investigates energetic and metabolic changes brought about by the genetic modification of the glucose uptake and phosphorylation system of *Escherichia coli.* The engineered strain PPA316, which lacks the *E. coli* phosphotransferase system (PTS) and uses instead the galactose-proton symport system for glucose uptake, exhibited significantly altered metabolic patterns relative to the parent strain PPA305 which retains PTS activity. Replacement of a PTS uptake system by the galactose-proton symport system is expected to lower the carbon flux to pyruvate in both aerobic and anaerobic cultivations. The extra energy cost in substrate uptake for the non-PTS strain PPA 316 had a greater effect on anaerobic specific growth rate, which was reduced by a factor of five relative to PPA 305, while PPA 316 reached a specific growth rate of 60% of that of the PTS strain under aerobic conditions. The maximal cell densities obtained with PPA 316 were approximately 8% higher than those of the PTS strain under aerobic conditions and 14% lower under anaerobic conditions. In vivo NMR results showed that the non-PTS strain possesses a dramatically different intracellular environment, as evidenced by lower levels of total sugar phosphate, NAD(H), nucleoside triphosphates and phosphoenolpyruvate, and higher levels of nucleoside diphosphates. The sugar phosphate compositions, as measured by extract NMR, were considerably different between these two strains. Data suggest that limitations in the rates of steps catalyzed by glucokinase, glyceraldehyde-3-phosphate dehydrogenase, phosphofructokinase, and pyruvate kinase may be responsible for the low overall rate of glucose metabolism in PPA316. © 1997 John Wiley & Sons, Inc. *Biotechnol Bioeng* **56:** 583–590, 1997.
Keywords: ^{31}P NMR; PTS mutant; *Escherichia coli;* metabolism; energetics; glucose uptake system; galactose symport system

* *Present address:* P.O. Box 4755, Bristol-Myers Squibb Company, Syracuse, NY 13221-4755.
Correspondence to: James E. Bailey
Contract grant sponsors: Advanced Industrial Concepts Division of the U.S. Department of Energy; National Science Foundation
Contract grant number: BCS 891284

INTRODUCTION

Metabolic engineering, which encompasses application of recombinant DNA technology to restructure metabolic networks for improvement of production of bioproducts (Bailey, 1991), provides many possibilities to optimize cellular functions for a particular application. In contrast to the precision that recombinant DNA techniques offer to change the cell genome at the molecular level, prediction of how cell physiology will respond to a genetic modification is much more difficult. This is due to the complexity of metabolic kinetics and regulation operating in a large number of reactions organized in branched and interacting pathways. Currently, exploratory experiments in metabolic engineering often lead to unexpected and undesired results. For example, abolishing both acetyl phosphotransferase (PTA) and acetate kinase (ACK) activities in an *Escherichia coli* strain resulted in accumulation of pyruvate as an unusual product (Diaz-Ricci et al., 1991). Mutation in the *ppc* gene coding for phosphoenolpyruvate carboxylase led to unwanted products, acetate and pyruvate (Miller et al., 1987).

Redirection of carbon flux distributions in primary metabolism may not be readily achieved because metabolic flux alterations are directly opposed by metabolic regulatory mechanisms which seek to maintain a flux distribution optimal for growth, not for overproduction of a particular metabolite (Stephanopoulos and Vallino, 1991). Therefore, in order to approach the goal of rational design of living cells for industrial applications and to advance knowledge about cellular regulation, systematic study is necessary to assess, in some detail, the metabolic consequences of specific genetic modifications for improving industrial microorganisms.

Although the effectiveness of genetic manipulation on a single pathway can be easily determined by simply measuring the target product, more complete assessment of the consequence of even a single mutation is not trivial. Mutation of a single gene or of its expression control can elicit

 CCC 0006-3592/97/050583-08

changes and responses not only directly associated with the gene product, but also in processes distant from the pathway in which the modification acts directly. In order to analyze the extent to which cell physiology has been changed and to gain insights useful in the next round of genetic modification, analysis should encompass details of the pathway of interest as well as interacting pathways.

In wild-type *E. coli* cells, glucose is transported into the cytoplasm through a group translocation mechanism by the phosphoenolpyruvate (PEP): carbohydrate phosphotransferase system (PTS), with concomitant phosphorylation using PEP as phosphorus donor, yielding glucose-6-phosphate (G6P) inside the cell (Fig. 1A, Postma et al., 1993). The present work explores the metabolic consequences of an alternative glucose uptake and phosphorylation system. This has the potential practical advantage of avoiding phosphoenolpyruvate depletion for glucose uptake, possibly making more carbon available for aromatic amino acid production. In particular, a strain has been constructed which uses a galactose-proton symport system for glucose uptake. As illustrated in Figure 1B, glucose phosphorylation in this mutant is ATP-dependent and catalyzed by the native *E. coli* glucokinase. A comparison of the PTS and symport systems shows other major differences between these two glucose transport schemes. The PTS system is energetically more efficient in the sense that only one high-energy phosphate bond is hydrolyzed during the process, while the symport system requires one high-energy phosphate bond *plus* one proton per each glucose molecule transported (Driessen et al., 1987). Also, there is a difference between these two systems in pyruvate coproduced: the PTS system couples glucose uptake with a stoichiometric coproduction of pyruvate and the symport system does not. Because pyruvate can either be channeled to the TCA cycle for energy production (under aerobic conditions) or further metabolized to acetate, succinate, lactate, ethanol, or other catabolic end products, it is expected that glucose metabolism downstream of pyruvate would be different in these two strains. Because intracellular energetic parameters such as ATP and transmembrane ΔpH participate in many intracellular regulations, any perturbation in these parameters could have profound influence on the entire metabolic network. Moreover, intracellular PEP concentration is also an important regulator in glycolysis through its roles in regulating phosphofructokinase (PFK), pyruvate kinase (PK), and PEP carboxylase, which connects glycolysis with TCA cycle.

We have investigated the energetics of these strains and the metabolic changes brought about by switching the glucose transport system. Bioreactor cultivations have been employed to assess the effects of the glucose uptake system on growth metabolism and associated fluxes of glucose and metabolic end products. Also, phosphorus-31 (^{31}P) nuclear magnetic resonance (NMR) spectroscopy has been applied to measure intracellular levels of nucleoside triphosphates (NTP), nucleoside diphosphates (NDP), and sugar phosphates (SP), while simultaneously determining the intracellular and extracellular pH values. Complementary to the whole-cell experiments, concentrations of phosphorylated intermediates in central carbon metabolism were measured from ^{31}P NMR spectra of perchloric acid (PCA) extracted cell samples.

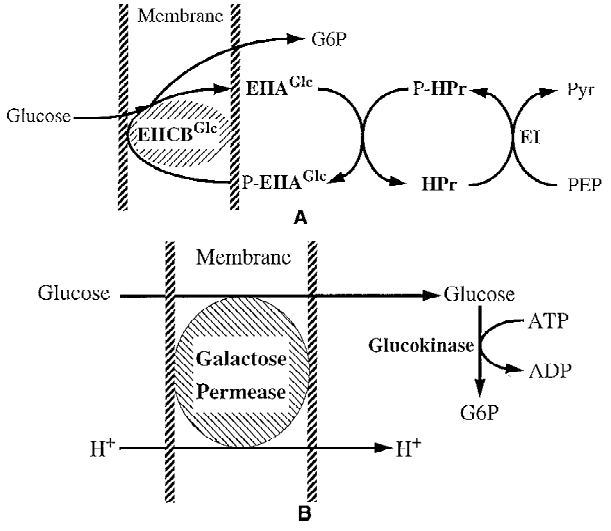

Figure 1. (A) A simplified schematic presentation of the phosphoenolpyruvate: glucose phosphotransferase (PTS) system in *E. coli.* HPr, EI, $EIIA^{Glc}$ and $EIICB^{Glc}$ denote enzymes involved in the glucose PT system. HPr and EI are the general PTS proteins. $EIIA^{Glc}$ and $EIICB^{Glc}$ are specific for glucose. Phospho-EII(glu), Phospho-HPr are the phosphorylated forms of enzyme IIA^{Glc} and enzyme HPr. (B) Schematic presentation of the galactose-proton symport system. Glucose, as well as galactose can be transported by this system.

MATERIALS AND METHODS

Strains

E. coli K-12 strain MG1655 was obtained from Carol Gross. PPA305 (*galP::*Tn*10*) was constructed via P1 transduction using *E. coli* UE 7 [*thi* Δ(*ptsH1-crr*)*galR galP::*Tn*10;* Boos et al., 1987] as donor and MG1655 as recipient. PPA309 [Δ(*ptsH1-crr*) *zfc-706::*Tn*10*] was derived from MG1655 by P1 transduction with a lysate of *E. coli* UE1 [*thi* Δ(*ptsH1-crr*) *zfc-706::*Tn*10 galR;* W. Boos, University of Konstanz, Germany]. Strain PPA316 [Δ(*ptsH1-crr*) *zfc-706::*Tn*10 galR*] was isolated from PPA309 by selecting for growth on glucose minimal plates.

Medium and Culture Conditions

The medium used in growth and metabolism studies contained (in grams per liter): glucose, 20; tryptone, 10; yeast extract, 5; Na_2HPO_4, 3; KH_2PO_4, 1.5; NaCl, 5. Cultivations were conducted in a 3.5 L (working volume 2 L) LH bioreactor (LH Fermentation, Hayward, CA). pH was controlled at 6.8 by adding 4 N NaOH. In aerobic experiments, the air flow rate was fixed at 2.0 L/min, and dissolved oxygen was controlled above 20% of air saturation by

manually adjusting agitation speed. Anaerobic conditions were maintained by flushing nitrogen into the bioreactor, with agitation speed set at 300 rpm. All cultivations were conducted at 37°C. The inocula were prepared with the same medium, and grown overnight at the same temperature, either in a shaker for aerobic experiments, or in a water bath for anaerobic experiments. In the latter case, nitrogen was flushed continuously through the flask, and agitation was driven by an external magnetic stirrer. One percent (V-V) inoculation was used in all cultivations.

Analytical Methods

The dry weight density of cell suspension taken from the bioreactor was measured. After two washes, the cell pellet was transferred to a pre-weighed aluminum plate which was dried at 105°C to constant weight. Metabolites in the supernatants were analyzed by high performance liquid chromatography (HPLC). A BioRad Aminex HXP-87H (300 × 7.8 mm) column was used, and 0.01N H_2PO_4 mobile phase at flow rate 0.4 mL/min was found to be satisfactory in resolving metabolites of interest. Glucose concentration in the medium was determined with a Sigma test kit (510-A). Ethanol and D-lactate were assayed using Boehringer-Mannheim kits. All absorbance measurements were made using a Shimadzu UV-260 Spectrophotometer.

NMR Whole Cell Experiments

Sample Preparations

E. coli cells were grown in 2-L shake-flasks in 1 L of M63 growth medium (3.0 g KH_2PO_4, 7.0 g K_2HPO_4, 2.0 g $(NH_4)_2SO_4$, 0.5 mg $FeSO_4$ per liter) supplemented with 5 g/L yeast extract. The cultivation of *E. coli* was carried out at 37°C and 275 rpm in a rotary shaker (New Brunswick Scientific). Glucose at an initial concentration of 5 g/L was used as the carbon source. Late-log phase cells were harvested by centrifugation at 7000 rpm using a JA-14 rotor for 5 min. This was followed by two washings using ice cold buffer containing: 100 m*M* Pipes (1,4-piperazinediethanesulfonic acid), 50 m*M* MES (2-[N-Morpholino]ethanesulfonic acid), 6 m*M* Na_2HPO_4, 6 m*M* KH_2PO_4, 60 m*M* NaCl, pH adjusted to 7.3. Afterwards, cells were suspended in the same buffer with the cell density of the sample cell suspension approximately 100 gDW/L [(grams dry weight)/L] for anaerobic NMR recording, or 40 gDW/L for aerobic samples to allow better oxygenation of the suspension. More accurate dry weight values, required to quantify intracellular concentrations, were measured by transferring the cell suspension after each experiment to a pre-weighed aluminum plate which was dried in a 105°C oven to constant weight. A 12.5 mL aliquot of the sample suspension was placed in a 20 mm (diameter) NMR sample tube, 1 mL D_2O was added as lock signal, and a sealed capillary with 0.1*M* methylene diphosphonic acid (MDP) was placed in the sample tube to provide a chemical shift reference. MDP resonates at 18.6 ppm downfield of 85% phosphoric acid which is assigned as 0 ppm.

^{31}P NMR Operations

^{31}P NMR experiments were performed on a Brucker AM300 NMR spectrometer in the Fourier transform mode at a frequency of 121.5 MHz. A 20 mm NMR broad-band probe was used. After adding 0.5 mL of glucose (500 g/L), spectra were accumulated in consecutive 1.5 minute blocks (120 transients), except where otherwise indicated, with a spectral width of 8000 Hz, and the free induction decays (FIDs) were sequentially stored on disk (8K). A pulse angle of 40° and relaxation delay of 0.2 seconds (recycle time) were used. Routine tuning, lock, and shimming were applied. All experiments were conducted at 25°C. A line broadening of 20 Hz was used in all the spectra from whole cell samples. At the end of each experiment, 80 μL phosphate (1*M*) was added to the sample, and spectra were taken for calibration purposes (Shanks, 1988).

PCA Extract NMR Experiments

Cell growth and harvest-washing-resuspension procedures were the same as for the whole cell experiments. After a desired elapsed time following glucose addition (until a quasi-steady-state metabolism is attained), 3.5 mL ice-cold perchloric acid (PCA; 70%) was added to the sample, 50 μL of MDP (1*M*) was also added to correct for any inaccuracy due to loss in the extraction procedure, and to provide a chemical shift reference. Samples were vigorously vortexed for 2 min at maximum speed. After resting on ice for 15 min, precipitates were removed by centrifugation in a desktop centrifuge at 2800 rpm for 15 min. Supernatants were neutralized with solid K_2CO_3, and precipitate was again removed by centrifugation. Extract was collected and diluted by a factor of 20, and pH was adjusted to 7.4. The resulting solution was passed through a Chelex 100 BioRad PolyPrep column (200–400 mesh) to remove paramagnetic cations. Post-ion exchange samples were frozen and then lyophilized using a LABCONCO freeze dry system.

For NMR spectroscopy of extracts, the lyophilized sample was redissolved in D_2O containing 20 m*M* EDTA of volume equal to the original sample volume. The samples were kept at −70°C until used in the NMR experiments. Samples were placed in 10-mm-diameter NMR tubes and ^{31}P NMR spectra were obtained on a Brucker AM 500 MHz spectrometer in the Fourier transform mode at a frequency of 202.49 MHz using a pulse angle of 90° and relaxation delay of 1 s. Free induction decays were accumulated for 1000 scans on 8K files. Composite pulse decoupling of protons was applied.

RESULTS AND DISCUSSION

This study examines the physiology of two strains designated: PPA305, which has a transposon insertion in the

galactose permease gene, and intakes glucose only via the PTS System; and PPA316, in which the PTS activity is deleted and intakes glucose using a constitutively expressed galactose permease. Strains PPA 305 and PPA 316 will also be referred to as the PTS and the non-PTS strains, respectively.

NMR Characterization

Figure 2 shows two typical ^{31}P NMR spectra for both strains in anaerobic quasi-steady states. This steady state is defined as a condition in which NMR-visible intracellular parameters such as total sugar phosphate, nucleoside triphosphate, and nicotinamide adenine dinucleotide [NAD(H)] concentrations estimated from successive NMR spectra do not change significantly. Under anaerobic conditions, PPA305 reached quasi-steady-state metabolism 5 min after the addition of glucose, during which time the resonances corresponding to NTP and SP increased quickly from zero and its initial level, respectively, to the steady-state conditions shown in Figure 2 (top spectrum). During the quasi-steady state, development of a pH difference across the cytoplasmic membrane was manifested by the appearance of the intracellular inorganic phosphate (P_i^{cyt}) peak as a downfield shoulder of the extracellular inorganic phosphate (P_i^{ex}) peak. The steady state lasted 10 min. PPA316 followed a similar trend, although it took 20 min to reach the quasi-steady state which lasted about 40 min.

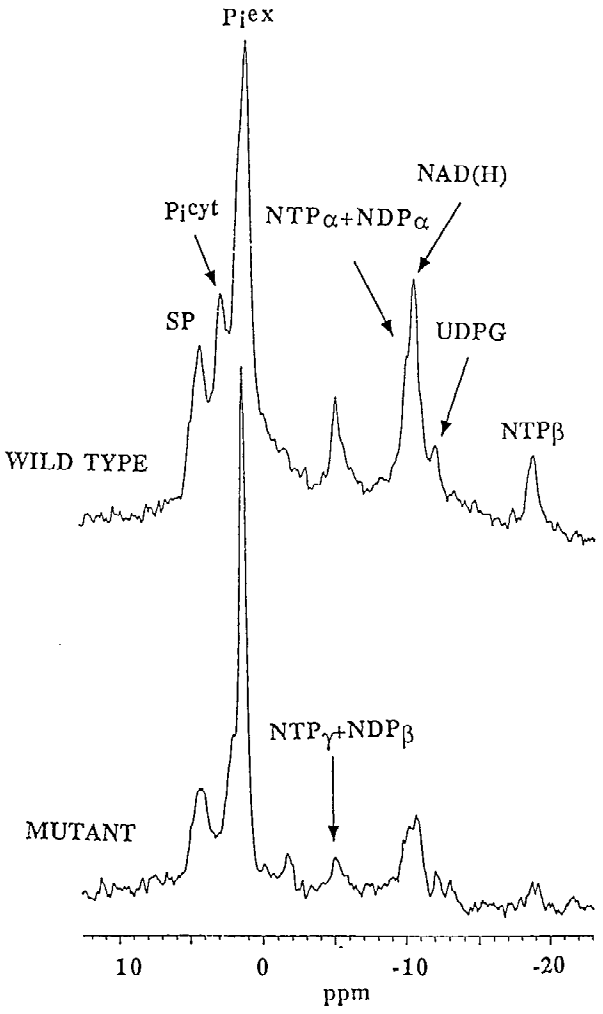

Figure 2. ^{31}P NMR spectra acquired during anaerobic glycolysis of *E. coli* strains PPA305 (top spectrum) and PPA316 (bottom spectrum). Spectra were obtained using 40° pulse and a relaxation delay of 0.2 s, other parameters as described in Materials and Methods. Abbreviations: SP: sugar phosphate; P_i^{cyt}: intracellular inorganic phosphate; P_i^{ex}: extracellular inorganic phosphate; NTP: nucleoside triphosphate; NDP: nucleoside diphosphate; NAD(H): nicotinamide adenine dinucleotide; UDPG: uridinediphosphoglucose.

The qualitative features of the spectra of both strains are very similar (Fig. 2) and are not different from those in the literature (Axe and Bailey, 1987; Diaz-Ricce et al., 1990; Ugurbil et al., 1978). Therefore, assignments of the peaks are based on these references. The resonances from 5 ppm to 3 ppm are in the sugar phosphate region (SP), which contains glucose-6-phosphate (G6P), fructose-6-phosphate (F6P), fructose-1,6-bisphosphate (FDP), 3-phosphoglycerate (3PGA) and 2-phosphoglycerate (2PGA), and other phosphorylated intermediates of glucose metabolism. Cytoplasmic inorganic phosphate P_i^{cyt} and extracellular inorganic phosphate P_i^{ex} are the next observable resonances. From their chemical shifts and a P_i-pH titration curve, pH values of both the cytoplasmic and the extracellular medium can be evaluated. The nucleoside resonances at −5, −10 and −18.6 ppm were assigned to NTP_γ + NDP_β, NTP_α + NDP_α and NTP_β, respectively. NAD(H), which includes both NAD^+ and NADH, appears at −11 ppm. UDPG and similar compounds resonate near −12 ppm.

For the PTS strain PPA305, 120 scans (acquisition time of 1.5 min) were sufficient to obtain a spectrum with reasonable signal-to-noise ratio. However, for the non-PTS strain PPA316, due to the much lower NTP level, more scans were needed to discern an NTP resonance above the noise. In order to compare NTP and NAD(H) levels, 4 individual assays (120 scans each) were summed. Figure 2 is one of the summed spectra (total 480 scans, total acquisition time of 6 min), and is scaled so that the levels of a given resonance can be directly compared. Therefore, the non-PTS strain has a very different intracellular environment compared to the PTS strain. This is manifested here in lower levels of total sugar phosphate, of the total concentration of NAD(H), of the high-energy compound NTP and in a much smaller ΔpH. The latter two are, of course, important energetic parameters.

Because inorganic phosphate is more abundant than NTP, the P_i peaks were resolved in each individual spectrum, and thus the pH in cytoplasmic and extracellular pH can be monitored with a time resolution of 1.5 min. Figure 3 shows the pH evolution for both the PTS and the non-PTS strains under anaerobic conditions. For PPA305, the extracellular pH decreased relatively rapidly compared to the extracellular pH change for PPA316. Under aerobic conditions, similar pH profiles were observed. Intracellular concentrations estimated from ^{31}P NMR data are given in Table I. In all

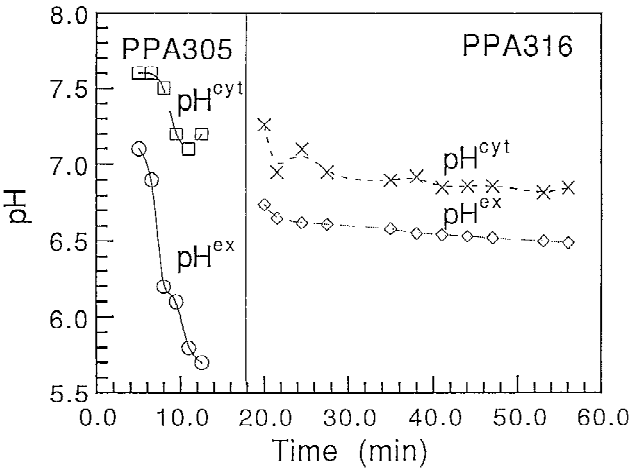

Figure 3. pH evolution of PPA305 (left part) and PPA316 (right part) during anaerobic glycolysis.

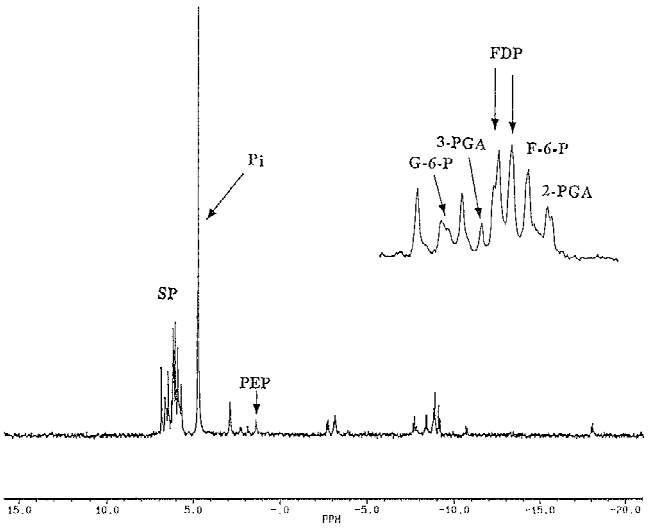

Figure 4. ^{31}P NMR proton decoupled spectra of PCA extract of PPA316. Spectra were obtained using 90° pulse and a relaxation delay of 1.0 s, other parameters as described in Materials and Methods. Abbreviations: P_i: inorganic phosphate; PEP: phosphoenolpyruvate. A line broadening (LB) of 2 Hz was used. Abbreviations in expanded SP region of the spectra: G-6-P: glucose-6-phosphate; F-6-P: fructose-6-phosphate; FDP: fructose-1,6-bisphosphate; 3-PGA: 3-phosphoglycerate; 2-PGA: 2-phosphoglycerate.

intracellular concentration calculations, an intracellular volume of 2.7 μL per mg of cell dry weight was assumed (Henderson et al., 1977), and concentrations were corrected for saturation effects due to fast pulses. Under both anaerobic and aerobic conditions, the non-PTS strain had a very low NTP level, about 0.8 m*M*, in contrast to 4.0 m*M* and 5.2 m*M* for the PTS strain under anaerobic and aerobic conditions, respectively. NDP concentrations can be evaluated by subtracting NTP_β from $NTP_\alpha + NDP_\alpha$. While the difference between these two resonance intensities was negligible for the PTS strain, indicating a very low concentration of NDP, the NDP for the non-PTS strain was estimated to be 0.2 m*M* under both anaerobic and aerobic conditions, indicating a greatly reduced energy charge.

The total nicotinamide adenine dinucleotide NAD(H) concentration was also substantially lower in the non-PTS strain, more so in anaerobic conditions. Ratios of SP levels in the PTS to those in non-PTS strain were 2.6 and 1.4 for aerobic and anaerobic glycolysis, respectively.

It appears that there is no simple correlation between the level of the total SP and rate of glucose metabolism. Therefore, ^{31}P NMR experiments on cell extracts were also conducted in order to examine the SP composition and measure PEP concentrations. Typical extract NMR spectra are shown in Figure 4. Many resonances resolved in the spectra were assigned by a combination of several methods. First tentative assignments were made based upon chemical shift values in the literature (Gadian et al., 1979; Robitaille et al., 1991), and these assignments were then checked by adding pure metabolites and taking additional spectra, or by pH titration. Quantitative results of sugar phosphate analyses of extract spectra are presented in Table II. The total concentrations of sugar phosphate agreed well with the estimates from whole-cell experiments, suggesting that artifacts of extract procedures as detailed in the Materials and Methods are not great. Any extract procedure suffers from some nonidealities; however differences between the two strains observed here, based on the same extract protocol, are clear.

In all cases, fructose phosphate (total concentration including both diphosphate and monophosphate) was the most abundant sugar phosphate, accounting for 68% and 76% of

Table I. Intracellular concentrations measured by ^{31}P NMR.[a]

	SP	NTP	NAD(H)	UDPG
		Aerobic condition		
PPA305	38	5.2	13	
PPA316	14	0.8	6.0	1.6
		Aerobic condition		
PPA305	39	4.0	15.0	
PPA316	28	0.8	5.4	2.8

[a]Concentrations are in m*M* and averages of at least three separate experiments.

Table II. S-P Concentrations measured by extract NMR.[a]

	Aerobic PPA305	Aerobic PPA316	Anaerobic PPA305	Anaerobic PPA316
G-6-P	1.2	1.5	2.1	0.7
3-PGA	1.3	0.6	1.3	1.0
FDP + F-6-P	26.	9.4	33.	18.
F-6-P	n.d.[b]	2.9	n.d.[b]	n.d.[b]
2-PGA	6.0	2.2	3.8	3.2
S-P-Un	3.9	2.5	3.3	5.6
S-P total	38.8	16.2	43.9	29.1
PEP	7.9	0.8	30.0	18.4

[a]Concentrations are in m*M* and are averages of at least three separate experiments. S-P-Un: unidentified sugar phosphate, other abbreviations are the same as Figure 5. The mean relative error: 20%.

[b]n.d. = not determined.

the total sugar phosphate in the PTS strain PPA305, under aerobic and anaerobic conditions, respectively. The percentages of fructose phosphate in PPA316 were similar: 76% under aerobic conditions and 62% under anaerobic conditions. The PEP concentration was much higher in the PTS strain, with a more pronounced difference compound to the non-PTS strain under aerobic conditions. For the other SP components, with one exception of G6P in aerobic conditions, PPA305 had higher values by a factor ranging 1.2 to 3. Consistent with our NMR data, an earlier NMR study showed that FDP was the dominating component found in the SP region; in some cases, up to 90% of SP was FDP (Ugurbil et al., 1978).

Metabolism and Growth Under Aerobic Conditions

The growth profiles and time courses of glucose and byproduct acetate concentrations in the medium for both strains are presented in Figure 5. The non-PTS strain PPA316 grew more slowly than the PTS strain PPA305. The specific growth rates in the exponential phase were 0.33 h^{-1} and 0.57 h^{-1} for PPA316 and PPA305, respectively. The maximal cell density obtained for PPA316 was 5.5 g/L (in dry weight), and PPA305 reached a slightly lower cell density, 5.1 g/L.

Of all the metabolites analyzed (acetate, ethanol, succinate, pyruvate, formate, and lactate), only acetate was accumulated in the growth medium at concentrations above detectable levels (0.05 g/L) for the PTS strain, consistent with earlier studies (Clark, 1989). Acetate concentration increased with the increase of cell concentration and began to level off at 8 h, when glucose concentration in the medium was low, reaching a maximal acetate concentration of 4.5 g/L. After the depletion of glucose, cells consumed acetate, and a slow increase of cell concentration was observed during this period. Neither acetate nor other metabolites were detected in the growth medium of the non-PTS strain. This is consistent with the difference in the maximal biomass concentrations obtained during growth, indicating that glucose was more efficiently used for biomass synthesis in the non-PTS strain because acetate excretion represents a waste of carbon. Avoiding acetate production allows a greater proportion of input carbon to flow to biosynthesis and/or a higher yield of cellular energy from glucose (in terms of ATP and/or proton motive force generation; Holms, 1986).

Previous studies suggest that acetate excretion is a consequence of a large flux to pyruvate (Holms, 1986). It follows that the non-PTS strain most likely has a smaller flux to pyruvate which prevented this overflow. In the non-PTS strain only pyruvate kinase (PK) converts phosphoenolpyruvate (PEP) to pyruvate. Our NMR data showed that the intracellular PEP concentration was significantly lower in cells of the non-PTS strain PPA316 than in the PTS strain (Table II), and this lower substrate concentration could, all else being equal, reduce the PK activity. A lower intracellular concentration of FDP also favors a smaller flux to pyruvate in this strain (FDP is a potent activator of PK).

Anaerobic Metabolism and Growth

Compared to the aerobic experiments, the difference in specific growth rates between the two strains studied was more significant. Differences in energetics between the two strains are expected to be more clearly manifested under anaerobic conditions in which only substrate-level phosphorylation produces ATP. As evident from Figure 6, the PTS strain grew 5 times as fast as the non-PTS strain, with a specific growth rate of 0.43 h^{-1}. The maximal biomass concentration obtained for PPA316 was 3.0 g/L, which was 0.5 g/L lower than observed for the PTS strain.

Figures 7a–e display time trajectories of fermentation products accumulated in the growth medium for both strains. Both strains produced acetate, ethanol, lactate, formate and succinate, to varying extents. Lactate was the only compound that was eventually produced in similar amounts in both strains (Fig. 7c), although the rates of lactate pro-

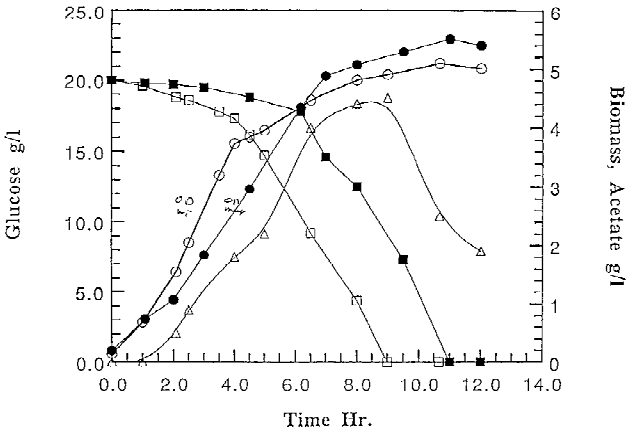

Figure 5. Time-trajectories of biomass, glucose and acetate during growth under aerobic conditions. Open symbols are for the PTS strain PPA305, solid symbols are for the non-PTS strain PPA316. (□), glucose; (○), biomass; (△), acetate.

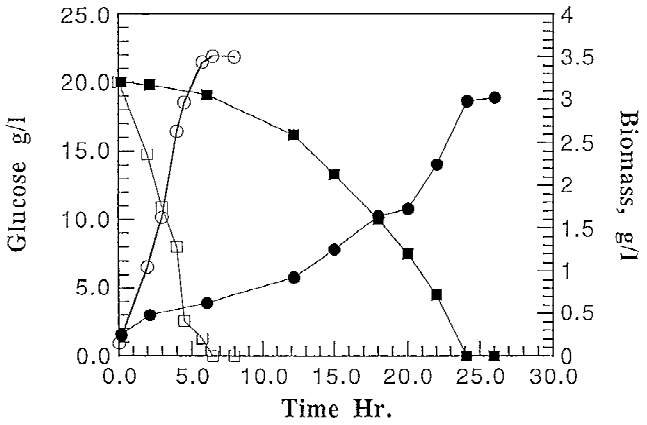

Figure 6. Time-trajectories of biomass and glucose under anaerobic conditions. Symbols are the same as Figure 5.

duction varied considerably. The profiles of ethanol were similar to those of acetate (Fig. 7a,b). The PTS strain produced approximately twice as much ethanol and acetate as the non-PTS strain. The net rate of formic acid accumulation was similar to those of lactate, acetate and ethanol for the PTS strain, but the non-PTS strain did not accumulate formate until the end of the cultivation, reaching a final concentration of 0.2 g/L, only 1/16 as high as that reached by the PTS strain. The non-PTS strain accumulated succinate in the later stage of the fermentation. The highest succinate concentration was 5.9 g/L, approximately 3.7 times higher than for the PTS strain.

In both growth and NMR studies, the non-PTS strain exhibited much lower rates of glucose catabolism. A limitation in the rate of glucose phosphorylation might be responsible for the lower rate of glucose catabolism in the non-PTS strain. Unfortunately, due to the minor role of glucokinase in glucose catabolism in wild-type strains, studies on glucokinase are scarce. The only reliable data on glucokinase concerns the enzyme from a related bacterium,

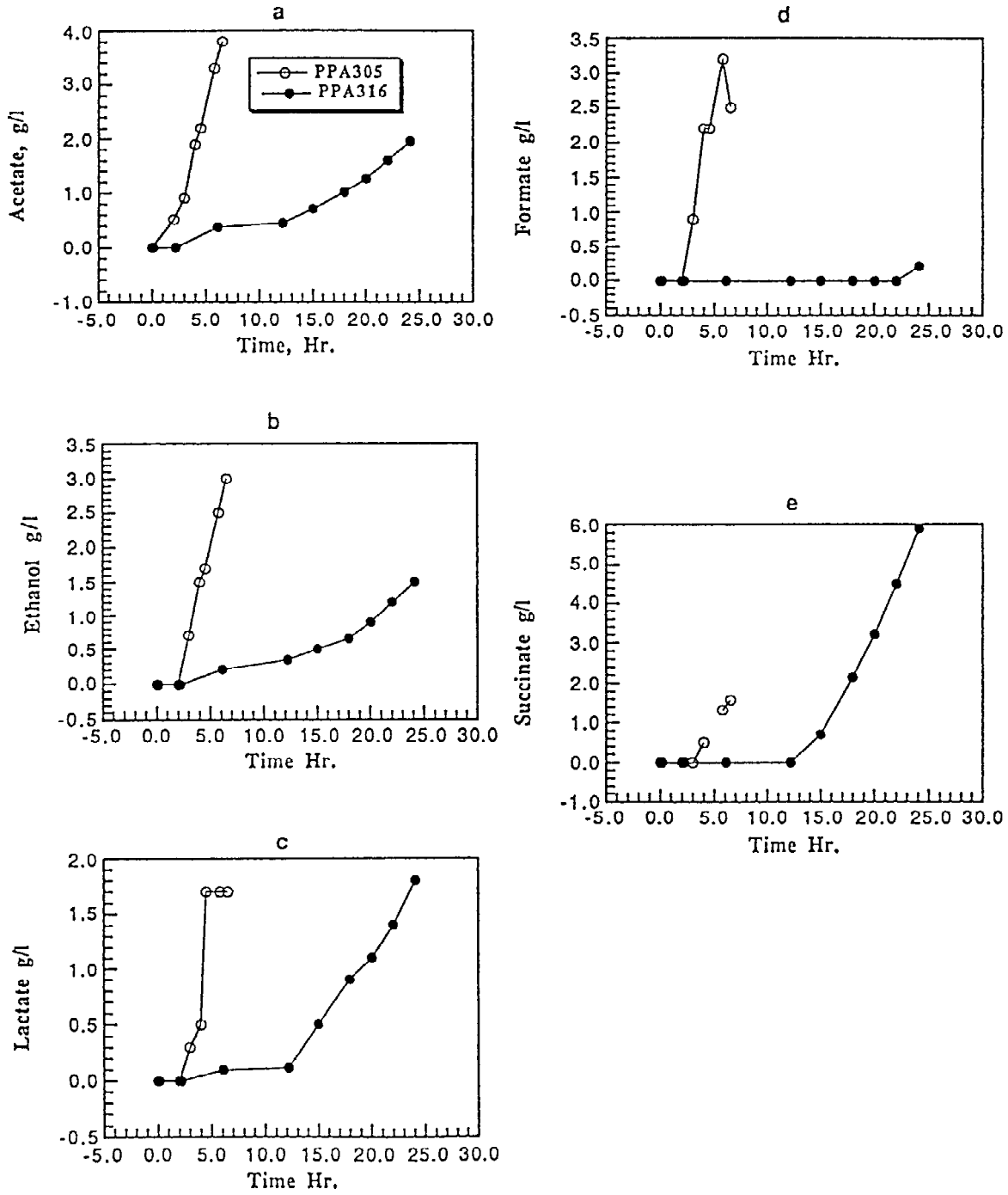

Figure 7. Evolutions of fermentation products in the supernatant during growth under anaerobic conditions. Open circles are for the PTS strain PPA305 and solid circles are for the non-PTS strain PPA316. (a) acetate, (b) ethanol, (c) lactate, (d) formate, (e) succinate.

Aerobacter aerogenes (Kamel et al., 1966); we will assume that the properties of this enzyme are similar to those in *E. coli*. The *A. aerogenes* glucokinase has a K_m for ATP of 0.8 m*M*. Our assays on the non-PTS strain indicate an NTP level of 0.8 m*M*, half of which can be reasonably assumed to be ATP (Lowry et al., 1971). Thus, ATP concentration may be limiting the phosphorylation of glucose by glucokinase.

Does any other part of the pathway also contribute to the low flux through the EMP pathway in the non-PTS strain? With unusually low ATP levels, and possibly low NAD^+ levels (based on a lower concentration of the total NAD(H) pool), it is possible that those reactions involving ATP and NAD^+ become rate-influencing steps. These reactions include glyceraldehyde-3-phosphate dehydrogenase and phosphofructokinase which use NAD^+ and ATP, respectively, as their substrates.

The LH BIOREACTOR and instrumentation were generously provided by LH Fermentation (Hayward, CA). The assistance of Dr. Robert Lee with the Bruker AM500 NMR spectrometer and of Dr. Vassily Hatzimanikatis with data analysis is greatly appreciated.

References

Axe, D. D., Bailey, J. E. 1987. Application of ^{31}P nuclear magnetic resonance spectroscopy to investigate plasmid effects on *Escherichia coli* metabolism. Biotechnol. Lett. **9**: 83–88.

Bailey, J. E. 1991. Toward a science of metabolic engineering. Science **252**: 1668–1674.

Boos, W., Ehman, U., Bremer, E., Midendorf, A., Postma, P. W. 1987. Trehalase of *Escherichia coli*. Mapping and cloning of its structural gene and identification of the enzyme as a periplasmic protein induced under high osmolarity growth conditions. J. Biol. Chem. **262**: 13212–13218.

Clark, D. P. 1989. The fermentation pathway of *Escherichia coli*. FEMS Microbiol. Rev. **63**: 223–234.

Diaz-Ricci, J. C., Hitzmann, B., Rinas, U., Bailey, J. E. 1990. Comparative studies of glucose catabolism by *Escherichia coli* grown in a complex medium under aerobic and anaerobic conditions. Biotechnol. Prog. **6**: 326–332.

Diaz-Ricci, J. C., Regan, L., Bailey, J. E. 1991. Effect of alteration of the acetic acid synthesis pathway on the fermentation pattern of *Escherichia coli*. Biotechnol. Bioeng. **38**: 1318–1324.

Driessen, M., Postma, P. W., van Dam, K. 1987. Energetics of glucose uptake in *Salmonella typhimurium*. Arch. Microbiol. **146**: 358–361.

Gadian, D. G., et al. 1979. Appendix 1: The ^{31}P chemical shifts of biological phosphorus compounds, measured as a function of pH, pp. 531–535. In: R. G. Shulman, (ed.), Biological applications of magnetic resonance. Academic Press, New York.

Henderson, P. J. F., Giddens, R. A., Jones-Mortimer, M. C. 1977. Transport of galactose, glucose and their molecular analogues by *Escherichia coli* K12. Biochem. J. **162**: 309–320.

Holms, W. H. 1986. The central metabolic pathways of *Escherichia coli:* Relationship between flux and control at a branch point, efficiency of conversion to biomass, and excretion of acetate. Current Topics in Cellular Regulation **28**: 69–105.

Kamel, M. Y., Allison, D. P., Anderson, R. L. 1966. Stereospecific D-glucokinase of *Aerobacter aerogenes*. J. Biol. Chem. **241**: 690–694.

Lowry, O. H., Carter, J., Ward, J. B., Glaser, L. 1971. The effect of carbon and nitrogen sources on the level of metabolic intermediates in *Escherichia coli*. J. Biol. Chem. **246**: 6511–6521.

Miller, J. E., Backman, K. C., O'Connor, M. J., Hatch, R. T. 1987. Production of phenylalanine and organic acids by phosphoenolpyruvate carboxylase-deficient mutants of *Escherichia coli*. J. Industrial Microbiol. **2**: 143–149.

Postma, P. W., Lengeler, J. W., Jacobson, G. R. 1993. Phosphoenolpyruvate phosphotransferase systems in bacteria. Microbiol. Rev. **57**: 543–594.

Robitaille, P. L., Robitaille, P. A. Brown, G. G. Jr., Brown, G. G. 1991. An analysis of the pH-dependent chemical-shift behavior of phosphorus-containing metabolites. J. Magn. Reson. **92**: 73–84.

Shanks, J. 1988. Metabolic engineering applications of *in vivo* ^{31}P and ^{13}C NMR studies of *Sacchromyces cerevisiae*. Ph.D. thesis, Caltech.

Stephanopoulos, G., Vallino, J. J. 1991. Network rigidity and metabolic engineering in metabolite overproduction. Science **252**: 1675–1681.

Ugurbil, K., Rottenberg, H., Glynn, P., Shulman, R. G. 1978. ^{31}P nuclear magnetic resonance studies of bioenergetics and glycolysis in anaerobic *Escherichia coli* cells. Proc. Natl. Acad. Sci. USA **75**: 2224–2248.